

Investigation of the toroidal dependence of first wall conditions in the Large Helical Device

T. Hino 1, 2), N. Ashikawa 1), Y. Yamauchi 2), Y. Nobuta 2), Y. Matsunaga 2), S. Masuzaki 1), A. Sagara 1), A. Komori 1) and LHD Experimental Group 1)

1) National Institute for Fusion Science, Toki, Gifu-ken, 509-5202 Japan

2) Lab. of Plasma Phys. and Eng., Hokkaido University, Sapporo, 060-8628 Japan

E-mail: tomhino @ qe.eng.hokudai.ac.jp

Abstract. The non-uniform wall conditions such as the fuel hydrogen retention and the erosion/deposition have been investigated in the Large Helical Device (LHD) by using toroidally and poloidally distributed material probes. They were installed in every experimental campaign from 2003 to 2010, and the evolutions of the wall conditions were clearly obtained. The wall conditions significantly depended on the operational procedures and the positions of in-vessel devices such as anodes for glow discharge and the ICRF antennas. The toroidal profiles for the amounts of retained hydrogen and helium, and the depth of wall erosion, were systematically measured. The hydrogen, helium and neon glow discharges have been conducted by using two anodes before and after the hydrogen or helium main discharges. The amount of retained hydrogen was large in the vicinity of the anodes, and drastically decreased as increase of the campaign number. This reduction well corresponds to the time period used for the hydrogen glow discharge conditioning. The erosion depth was large at the walls relatively close to the anodes, which is owing to the sputtering during the helium and neon glow discharges. The depositions of carbon and boron also depended on the positions of NBI and diborane gas inlet used for boronization, respectively. The amount of the retained helium was large at the walls close to the anodes owing to the helium glow discharge. The amount of retained helium became large at the walls close to the ICRF antennas owing to the implantation of high energy helium during the helium main discharge with the ICRF heating. In the present study, the toroidal dependences of the gas retention and the erosion/deposition in LHD were obtained, and the effects of the in-vessel devices on these plasma wall interactions were clarified.

1. Introduction

It is important to know the wall conditions of fusion devices and their changes arising from the progress of plasma discharge experiments. Information on the fuel hydrogen retention, wall erosion and the impurity deposition on plasma facing walls are required to understand the impurity behavior in the plasma and the degree of fuel gas recycling. For this purpose, numerous material probes were installed in every experimental campaign in LHD since 1998, and the surface properties of the material probes such as gas retention, atomic composition and surface morphology were analyzed after the campaign [1]. Then, the wall condition data were systematically accumulated as a database, and used to construct the experimental plan of the next experimental campaigns.

From the first campaign, five material probes were installed along the poloidal direction at toroidal sector of 7 as shown in *FIG. 1*, to investigate the poloidal dependence of the plasma wall interactions [1]. In the first campaign, He ECR discharge cleaning was employed for the initial ECH plasma production. H₂ and He glow discharge cleanings were used from the 2nd campaign for the production of NBI heated main discharges. The material probe analyses showed that the impurity of Fe-O at the wall surface was significantly reduced by these glow discharges. From the 3rd campaign, for ICRF heated plasmas and high power plasma production, graphite tiles were installed in the divertor leg region. The radiation loss owing to the iron in the plasma was significantly reduced. The plasma stored energy drastically increased by the reduction of the radiation loss and the increase of the heating power. The material probe analyses showed that the carbon deposition was thick at the walls far from the plasma (#4 and #5). The amount of retained hydrogen and helium was also large at these walls. At the other walls (#1 - #3), thin carbon deposition was observed. The plasma performance well agreed with the change of the wall conditions obtained by the material probe analyses.

Improved plasma performance was investigated in the 4th campaign, relevant mainly to the magnetic axis position. The plasma stored energy exceeded 1 MJ. After the 6th campaign, in addition to H₂ and He glow discharges, Ar and Ne glow discharges were newly employed to reduce both the fuel hydrogen and helium retentions. The low density discharge with a high ion temperature became possible after Ar and/or Ne glow discharge conditionings. The plasma performance improved very well owing to both this conditionings and the increase of the heating power [2]. The ion temperature has reached 5.2 keV at the density of $1.6 \times 10^{19} \text{ m}^{-3}$. The super high density plasma was obtained by the formation of internal diffusion barrier (IDB) owing to the pellet injection. The central density has exceeded $1 \times 10^{21} \text{ m}^{-3}$. The average plasma beta exceeded 5% and the plasma stored energy reached to 1.6 MJ as shown in *FIG. 2*.

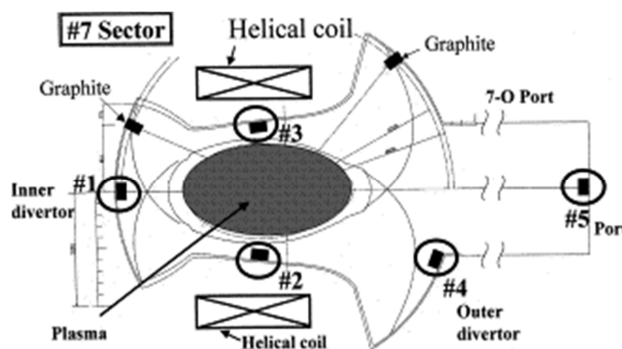


FIG. 1 Position of material probes at the inner wall of toroidal sector #7.

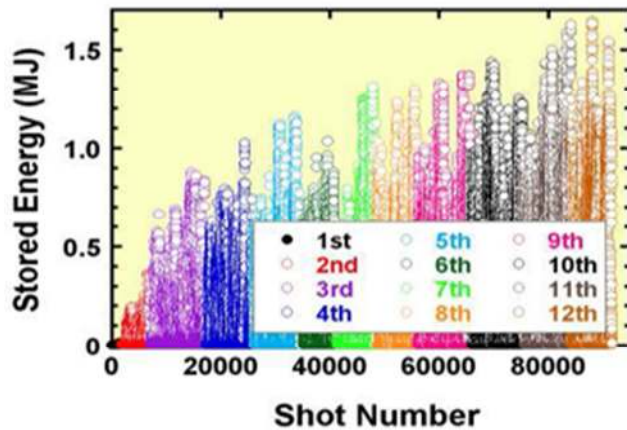


FIG. 2 Increase in the plasma stored energy with shot number.

From the 4th campaign, in addition to the poloidally located five material probes, ten material probes were installed along the toroidal direction as shown in FIG. 3 to elapse the toroidal dependence of the plasma wall interactions [3]. In particular, it is important to know the changes of fuel hydrogen retention, the wall erosion and the impurity deposition, since the Ar and Ne glow discharges were newly applied after the 4th campaign. The poloidal location of these probes was at the bottom of first wall (#2 in FIG. 1). The holder for the material probe, for example, in the 11th campaign, contained three probes, two SS samples and one Si sample, as shown in FIG. 4. The SS samples were used to measure the gas retention by thermal desorption spectroscopy (TDS) and to observe the change of surface morphology by scanning electron microscope (SEM). The half of Si sheet was coated by B film to measure the wall erosion. The non-coated region in the Si sample was used to measure the deposition of impurities such as C and B by using Auger electron spectroscopy (AES).

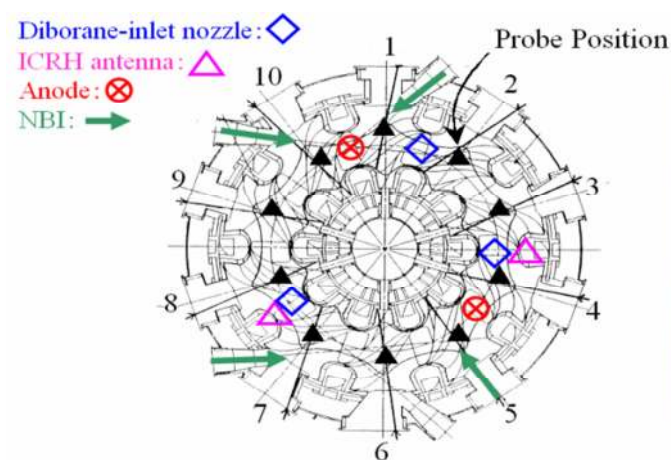


FIG. 3 Toroidal location of material probes.



FIG. 4 Material probe holder installed in the 11th campaign.

2. Toroidal dependences of wall erosion and impurity deposition

We here look the results of the material probe analyses obtained for the 11th campaign. This campaign was conducted from Oct. in 2007 to Feb. in 2008. The numbers of hydrogen and helium main discharges were 6300 and 2400 shots, respectively. Total time periods for the H₂, He and Ne glow discharges were 168, 152 and 72 hours, respectively. The boronization using (B₂H₆ + He) glow discharge was twice conducted in Sept. of 2007 and Feb. in 2008.

The eroded thickness of B film on the Si probe in the 11th campaign was measured using both a surface roughness meter and the etching time of Ar ion in AES analysis. The toroidal profile of eroded thickness for B film is shown in *FIG.5*. The eroded depth was large in the vicinity of the anodes used for the glow discharge. The Ne glow discharge was conducted in addition to the He glow discharge in this campaign. The sputtering yield of neon ion is a few times larger than that of helium ion. Thus, the erosion became dominant at the walls close to the anodes. The contribution of the main discharge on the erosion was relatively smaller, compared with that of the glow discharge. This result indicates that the high ion current density in the glow discharge contributed to the erosion. *FIG.6* shows the thickness of impurity layer deposited on Si probe without B coating in the 11th campaign. The thick deposition of boron was observed at the toroidal sector 1, where the inlet nozzle of diborane gas was close to the anode. The densities of the ion and the neutral radical containing boron become high in this position, and thus the boron thickness becomes large. The carbon deposition was observed at every toroidal position, in particular dominant at the toroidal sector 10. The high power NBI was conducted around this region, and then a lot of carbon impurity might have been transported from the graphite divertor tiles during the main discharges.

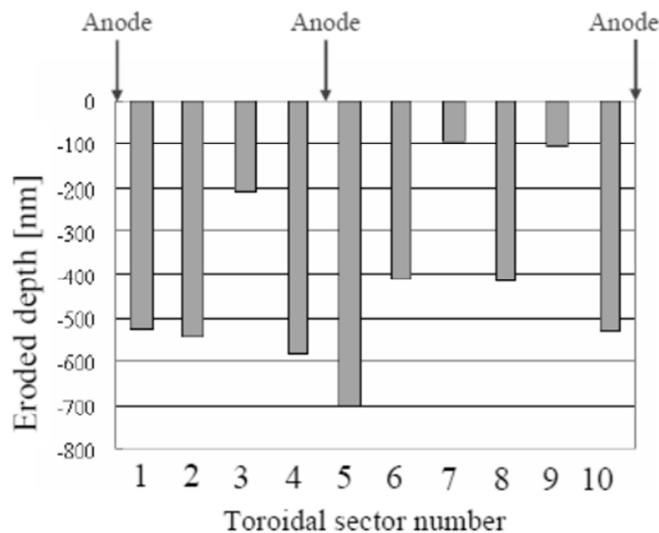


FIG.5 Toroidal dependence of eroded depth in the 11th campaign.

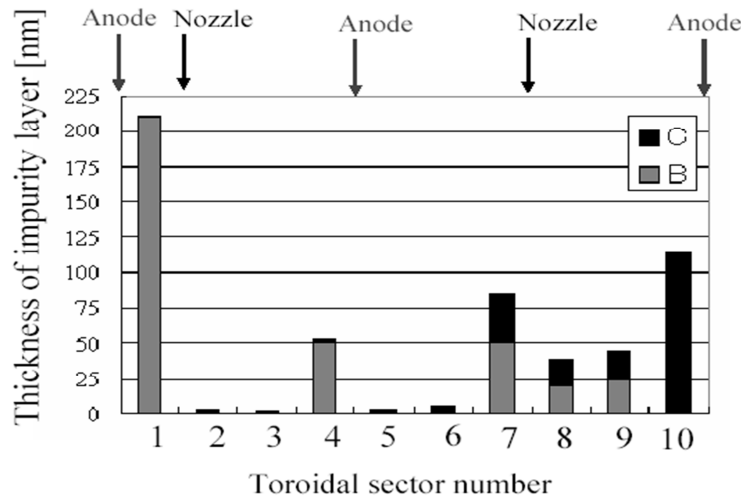


FIG.6 Toroidal dependence of deposition thickness in the 11th campaign.

3. Toroidal dependence of fuel hydrogen retention

The amount of retained hydrogen was obtained by TDS analysis for the SS probes, which is shown in FIG.7. It is seen that the amount of retained hydrogen was large in the wall close to the anodes. This result suggests that the hydrogen was retained mainly during the H₂ glow discharges, not during the hydrogen main discharges. In addition, the amount of retained hydrogen decreased as increase of the campaign number. In particular, the values in the 10th and 11th campaigns were very small. The reason is a short time period for the H₂ glow discharge as shown in FIG.8. It is noted that the amount of retained hydrogen was large in the 6th campaign though the time period of H₂ glow discharge was short. This reason is due to that the H₂ glow discharge was conducted in the final stage of the campaign. As described above, the deposited thicknesses of boron and carbon were large at the toroidal sectors 1 and 10, respectively. The amounts of retained hydrogen were also large at these sectors. In the 9th and 10th campaigns, similar results were obtained. This behavior may be understood that the boron or the carbon well retains the hydrogen.

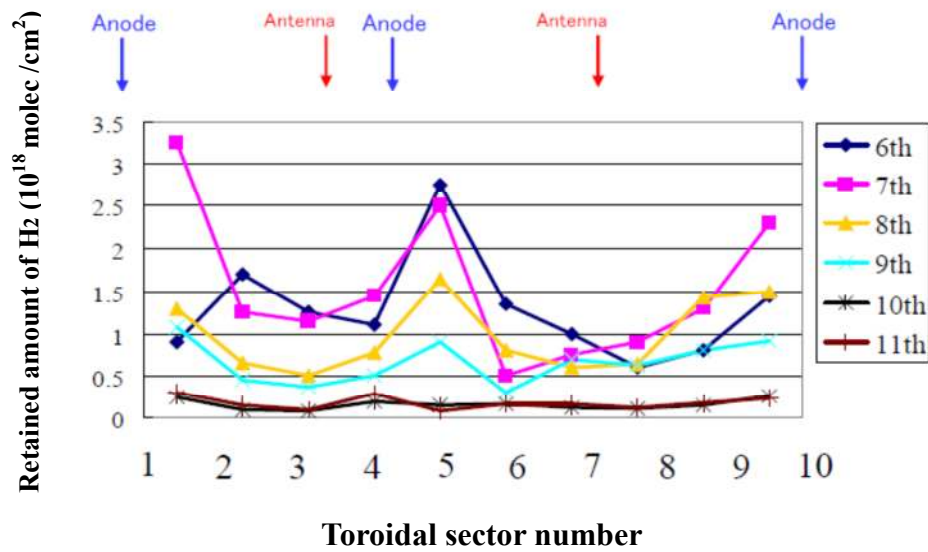


FIG. 7 Toroidal dependence of amount of retained of hydrogen.

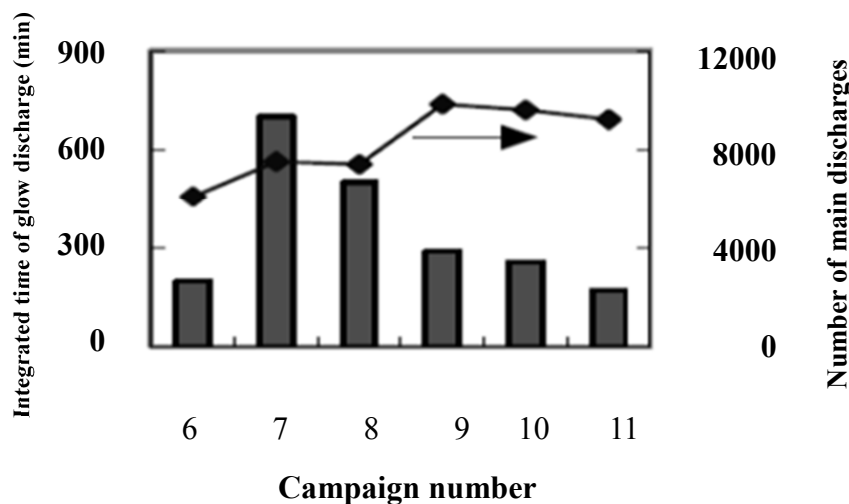


FIG.8 Time period for hydrogen glow discharge vs campaign number.

4. Toroidal dependence of helium retention

The glow discharge and the main discharge using He have been conducted in LHD. It was seen that the amount of retained helium was not negligible, only one or two orders of magnitude smaller than that of hydrogen [1, 3]. Thus, the mechanics for the helium trapping has to be clarified. For this purpose, the SS samples exposed to only the glow discharges and only the main discharges were prepared at the wall far from the plasma (#5 in FIG.1), by using the sample holder with a shutter [1]. FIG.9 shows the helium desorption spectra for the samples exposed to only the glow discharges and only the main discharges. The helium desorbed mainly in the temperature regimes lower than 900 K and higher than 900 K in the samples exposed to only glow discharges and main discharges, respectively. The energies of helium ion in the glow discharge and the main discharge are several

hundred eV and (1-2) keV, respectively. The blister produced by the implantation of helium ion with a lower energy during the glow discharge is smaller and shallower than that with a higher energy during the main discharge. This may be the reason that the helium desorbed at the lower temperature regime in the sample exposed to only the glow discharge.

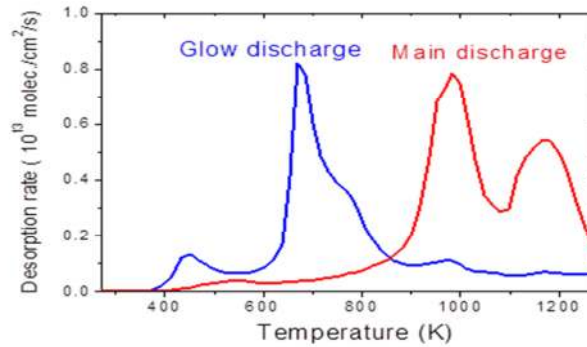


FIG.9 Helium desorption spectra for the SS samples exposed to only glow discharges and only main discharges.

FIG.10 shows the toroidal profile for the amount of retained helium in the 7th campaign. In this campaign, the ICRF heating was not conducted. The amount of retained helium was large at the walls close to the anodes. The retention of helium during the helium glow discharges was dominant compared with that during the helium main discharges, around at the wall close to the anodes. At the walls far from the anodes, the contribution by the helium main discharge was roughly comparable with that by the helium glow discharges. The toroidal profiles for the amount of retained helium in the 9th, the 10th and the 11th campaigns with the ICRF heating are shown in FIG.11. The amount of retained helium was large at the walls close both the anodes and the ICRF antennas. In the 10th and the 11th campaigns, the amount desorbed at the temperature higher than 900 K was large at the walls close to the ICRF antennas. This indicates that the helium with energy of several keV in the helium main discharge was retained at the walls close to the antennas during the ICRF heating.

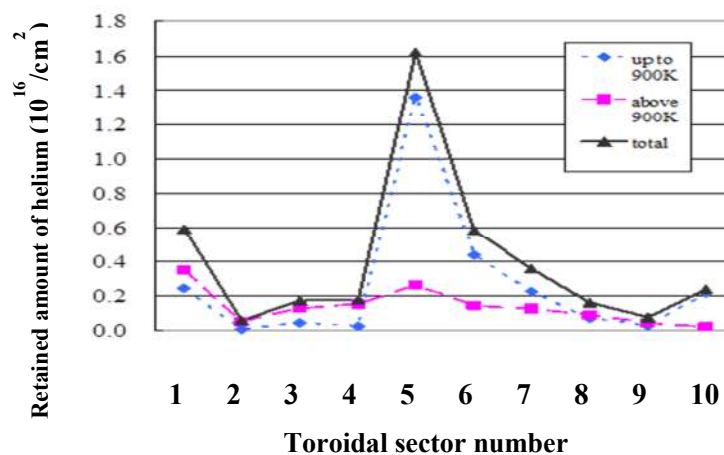


FIG.10 Toroidal profile for amount of retained helium in 7th campaign.

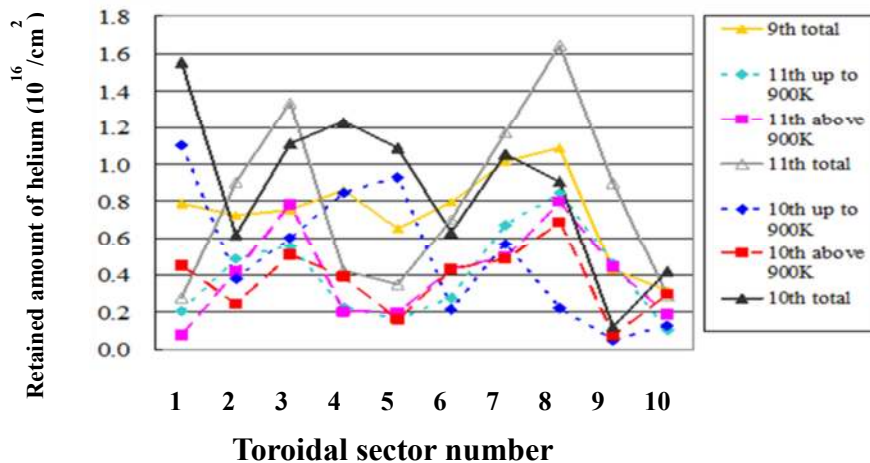


FIG.11 Toroidal profiles for amount of retained helium in 9th, 10th and 11th campaigns.

4. Conclusion

In summary, the wall behavior in LHD was investigated by using the material probe technique. The amount of retained hydrogen was large at the wall close to the anodes used for the glow discharge. The erosion was dominant at the wall close to the anodes. It is clearly shown that the glow discharge significantly contributed both to the hydrogen retention and the wall erosion. The positional dependence of impurity deposition was also investigated. Major species of deposited impurities were B and C, and the deposited amounts depended on the positions of gas inlet for diborane and NBI heating, respectively. The amount of retained hydrogen in the walls with a thick deposition of B or C was large. The amount of retained helium was large at the walls close to the anodes. In the campaigns with ICRF heating, the amount of retained helium became large at the walls close to the antennas, owing to the trapping of high energy helium during the helium main discharges. In the present study, the positional dependence of the wall conditions was systematically obtained. These results significantly contribute to make an experimental plan for the next experimental campaign.

Acknowledgement

This work is supported by the Collaboration Study Program of National Institute for Fusion Science (NIFS06KLPP301).

References

- [1] Hino T. et al, Nucl. Fusion **44** (2004) 496
- [2] Komori A. et al, Nucl. Fusion **49** (2009) 104015
- [3] Hino T., et al, Fusion Eng. and Design **82** (2007) 1621